Physically-Based High-Level System Model of a MEMS-Gyroscope for the Efficient Design of Control Algorithms

Ruslan Khalilyulin, Gabriele Schrag, Gerhard Wachutka

Institute for Physics of Electrotechnology, Munich University of Technology, Arcisstrasse 21, 80290 Munich, Germany
Phone: +49-89-28923128, Fax: +49-89-289-23134, ruslan@tep.ei.tum.de

ABSTRACT

We present a high-level model of a dual gimbaled mass gyroscope, which provides an accurate physical description of the impact of external and internal disturbances on the output signal, but which also allows for the efficient analysis and optimization of the full sensor system including the electronic circuitry for drive, control, and signal conditioning. The dynamics of the gyroscope is described by a reduced-order high-level model. Internal disturbances (manufacturing tolerances, e.g.) as well as external impact factors (pressure-dependent viscous damping, shock, vibrations of the housing, etc.) are included in the model equations by introducing physically-based, parameterized functions extracted from detailed FEM or mixed-level simulations. Exemplary simulations investigating the impact of package vibrations on the sensor output signal prove the efficiency of our model and the practicality of our approach.

1 INTRODUCTION

Robust sensor systems designed for applications in harsh environments (e.g., automobiles) have to be equipped with additional "smart functionalities" to compensate environ mental impacts (e.g., ambient pressure variations or package vibrations) or internal imperfections due to manufacturing tolerances.

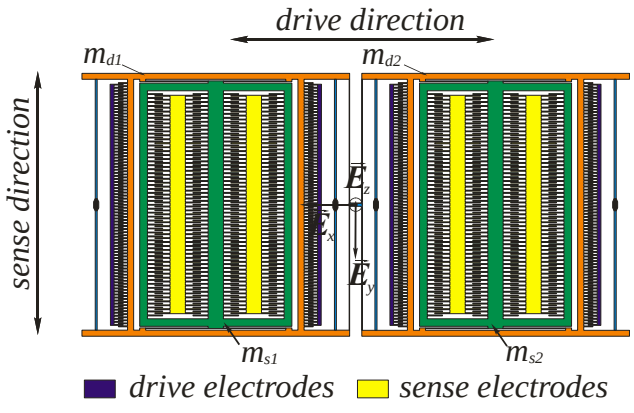

Fig. 1: Structure of the dual gimbaled mass gyroscope.

In order to ensure a proper and reliable sensor operation, adequate concepts for sensor control and signal conditioning must be developed, which are based on a profound understanding of the effects disturbing the sensor output signal. To this end, we derived a high-level model of the dual gimbaled mass gyroscope depicted in Fig. 1, which provides an accurate physical description of the impact of external and internal disturbances on the output signal, but, at the same time, allows for the efficient analysis and optimization of the full sensor system including the electronic circuitry for drive, control, and signal conditioning and, thus, is perfectly suited for the co-design of the transducer elements and the control electronics

2 HIGH-LEVEL GYROSCOPE MODEL

2.1 Modeling Approach

As it would be much too time- and memory-consuming to perform a complete continuous-field FEM analysis of the gyroscope including all possible mechanical configura tions, we focus on the most relevant modes of motion and decompose the device structure into four rigidly moving

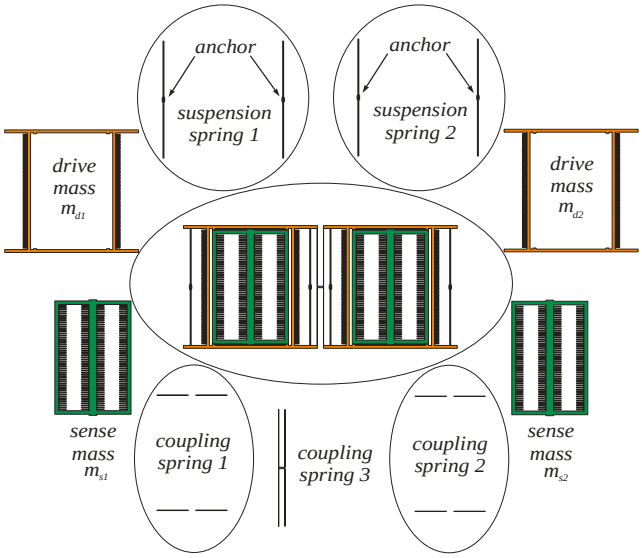

Fig. 2: Decomposition of the gyroscope into four rigidly moving bodies connected by mass-less springs.

mechanical substructures, which are hinged and inter linked by springs (Fig. 2). The dynamics of this simplified structure is described by the Langrangian equations of motion, leading to a reduced-order model of the complete gyroscope with 24 degrees of freedom [1]:

$$\begin{aligned} &\boldsymbol{M}\cdot\ddot{\underline{u}}+(\boldsymbol{C}+\boldsymbol{C}_{\Omega})\cdot\dot{\underline{u}}+(\boldsymbol{K}+\boldsymbol{K}_{\Omega})\cdot\underline{u} \;= \\ &= -\boldsymbol{M}\cdot\underline{a}_o+\underline{F}_{el} \end{aligned} \tag{1}$$

Here $\boldsymbol{K}$ and $\boldsymbol{M}$ denote the stiffness and the mass matrices, $\boldsymbol{C}$ the damping matrix**,** which accounts for viscous friction due to the surrounding air, $\underline{F}_{el}$ the electrostatic forces actuating the drive masses, and $\underline{a}_0$ the external linear acceleration acting on the substrate frame. The measurand, the angular velocity $\vec{\Omega}$, enters the system through the terms $\boldsymbol{C}_{\Omega}$ and $\boldsymbol{K}_{\Omega}$, which comprise the contributions of the Coriolis and the centrifugal force to the stiffness and the damping matrix, respectively.

2.2 Mechanical Model Parameters

The mechanical model parameters like the mass matrix $\boldsymbol{M}$ and the stiffness matrix $\boldsymbol{K}$ were extracted from detailed 3D FEM simulations by calculating the respective inertial forces and spring constants for each rotational and translational degree of freedom. The three fundamental resonance frequencies and the associated mode shapes of the gyroscope as obtained from the harmonic solutions of the homogeneous equation system (1) (i.e. $\underline{a}_o = 0$, $\underline{F}_{el} = 0$) conform well with those calculated by modal FEM analysis (see Fig. 3 and Tab. 1).

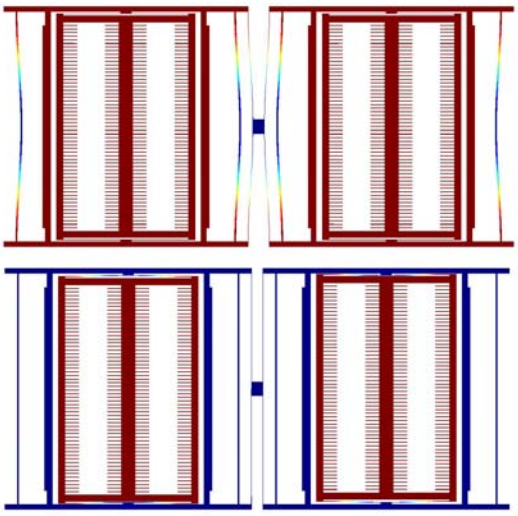

Fig. 3: Results of FEM modal analysis of the gyroscope structure.
Top: anti-phase drive mode at 10.654 kHz
Bottom: sense mode at 10.527 kHz

Resonance frequencies of the gyroscope	***FEM***	***harmonic solution***
in-phase drive mode	*10.301 kHz*	*10.459 kHz*
sense mode	*10.527 kHz*	*10.677 kHz*
anti-phase drive mode	*10.654 kHz*	*10.723 kHz*

Table 1: Three fundamental mechanical resonance frequencies of the gyroscope.

It shows that manufacturing fluctuations such as, e.g., etch bias tolerances have a considerable impact on the mass and stiffness parameters.

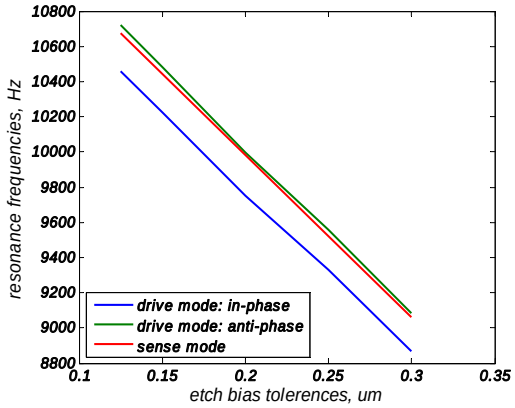

Fig. 4: Impact of manufacturing tolerances on the resonance frequencies of the drive and the sense masses.

The dependencies from these parameter variations have been analyzed (see Fig. 4) and extracted by detailed FEM simulations and, subsequently, fed into the high-level model as parametrized functions.

2.3 Viscous Damping Model

Viscous damping due to the surrounding air is, by its nature, a distributed effect, which cannot be properly described by analytical compact models and which is also difficult to extract from 3D coupled-domain FEM simulations, especially for geometrically complex microstructures. Therefore, we included this effect by introducing modal quality factors $\hat{C}_i$ for all relevant modes of motion:

$$\hat{C}_i = \frac{\sqrt{\hat{K}_i \cdot \hat{M}_i}}{\hat{Q}_i} \tag{2}$$

where $\hat{K}_i$, $\hat{M}_i$ and $\hat{Q}_i$ denote the stiffness, mass and quality factors of the *i*-th eigenmode, respectively. The $\hat{C}_i$ are then converted into the spatial damping matrix $\boldsymbol{C}$ by applying modal transformation techniques.

NSTI-Nanotech 2008, www.nsti.org, ISBN 978-1-4200-8505-1 Vol. 3

Since it is computationally quite expensive and for the required accuracy of the system model also not necessary to determine the quality factors for a large number of eigenmodes, we focussed on the two most relevant modes of motion, i.e. the sense mode, which is mainly affected by squeeze film damping, and the drive mode, whose dynamics is dominated by slide film damping.
In detail, the modal quality factor of the drive mode can be determined by:

$$\frac{1}{Q_{drive}} = \frac{1}{Q_{sl\_fr}} + \frac{1}{Q_{comb}} \tag{3}$$

where Q_{sl_fr} represents the quality factor of the drive and sense frames and Q_{comb} the quality factor of the comb drives. For the calculation of both quality factors we apply the following expression for slide film damping given in [2]:

$$Q_i = \frac{\hat{M}_i \cdot \omega_i \cdot h}{\eta_{eff} \cdot A_{eff}} \tag{4}$$

Here ω_i stands for the angular eigenfrequency of the *i*-th eigenmode (drive frequency), h for the distance between the moving frame and the substrate or, alternatively, the distance between the comb fingers, A_{eff} for the relevant effective area, and η_{eff} is the effective viscosity accounting for gas rarefaction effects in the low pressure regime and/or small structural dimensions [2]:

$$\eta_{eff} = \frac{\eta_T}{1 + 2 \cdot K_n + 0.2 \cdot K_n^{0.788} e^{-Kn/10}} \tag{5}$$

(with η_T = viscosity of air under normal pressure conditions at room temperature and K_n = Knudsen number).
The modal quality factor of the sense mode is dominated by squeeze film damping and was determined by applying the mixed-level modeling approach proposed in [3]. This approach takes advantage from the small Reynolds numbers and the large aspect ratios typically encountered in MEMS structures and reduces the degree of complexity by replacing the non-linear and highly complicated Navier-Stokes equation by the well-known Reynolds' equation [4]:

$$\nabla\left(\frac{\rho h^3}{12\eta_{eff}} \nabla p(x,y)\right) = \frac{\partial}{\partial t}(\rho h) \tag{6}$$

The pressure distribution *p(x,y)* underneath the moving plates is calculated by discretizing this equation to form a fluidic Kirchhoffian network and solving it by the use of a standard circuit simulator. Edge effects and perforations in the structure are taken into account by introducing physically-based compact models at the respective locations. The pressure-dependent quality factors of the sense mode, as they have been extracted from these mixed-level simulations and incorporated in the high-level model, are shown in Fig. 5.

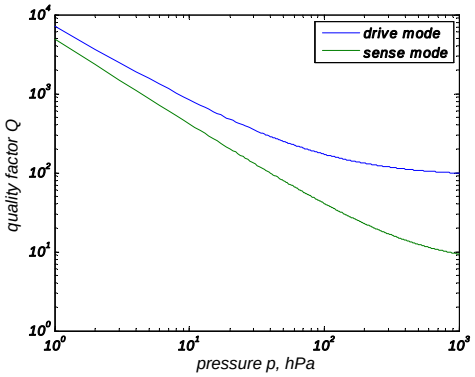

Fig. 5: Pressure-dependent quality factors of the drive and the sense mode of the gyroscope.

3 IMPACT OF ENVIRONMENTAL DISTURBANCES ON THE SENSOR SYSTEM

By their nature, inertial sensors are sensitive to any kind of mechanical forces originating from their environment. Thus, their operation is always affected by disturbing effects arising under real-world operating conditions like shock, cross-talk between sensing and non-sensing axes, and vibrations of the housing. These impact factors enter our sensor model in a physically transparent manner through the parameters $\boldsymbol{C_\Omega}$ and $\boldsymbol{K_\Omega}$ and the right-hand side of the model equations, respectively; hence, it provides the proper basis for studying their influence on the sensor system on the whole and, therefore, it is well suited for the design of adaptive control algorithms, which minimize or even eliminate the environmental disturbances.
As an example, we demonstrate the efficiency of our high-level model by analyzing the impact of housing vibrations on the transient sensor response. To this end, we first consider the package alone and extract its eigenmodes and resonance frequencies from FEM calculations [1]. Tab. 2 shows the results for two exemplary standard package types (PSOIC and QFP).

		PSOIC	*QFP*
in-plane	*x-direction*	*14.654 kHz*	*30.379 kHz*
in-plane	*y-direction*	*14.835 kHz*	*30.387 kHz*
out-of-plane	*z-direction*	*25.666 kHz*	*43.656 kHz*

Table 2: Vibration modes of the PSOIC and QFP packages

The interface circuitry of the gyroscope system has been designed as a digital self-oscillation loop based on Δ-Σ-modulation (see Fig. 6). Among others, it ensures the proper operation of the gyroscope by forcing the drive masses to operate in anti-phase mode.

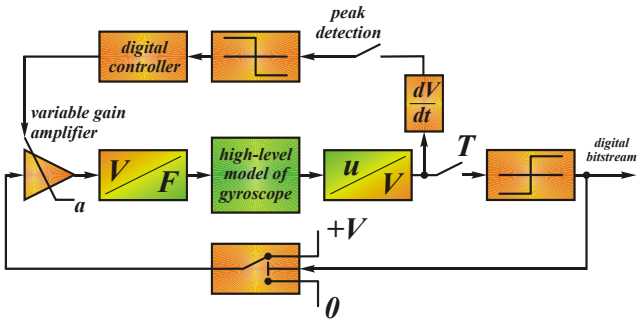

Fig. 6: Block diagram of the drive control loop.

For the compensation of disturbances a so-called "Automatic Gain Control (AGC)" algorithm has been implemented. The basic idea of this approach is to introduce an externally controlled term proportional to $\dot{\underline{u}}$ in the friction force in order to control the oscillation velocity of the drive masses and to adjust it to a constant value [5].

The package vibrations enter the model of the gyroscope system through the term $\underline{a}_0$ in eq. (1). Since the strongest impact on the sensor output signal is to be expected from those vibration modes, which have the same vibration direction as the sense masses, i.e. the y-direction, only these quantities are fed into the gyroscope model, assuming that the vibrations of the package are transferred to the gyroscope without damping losses.

An important result of a full system analysis is that the device loses the ability to compensate the disturbing package vibrations if, due to manufacturing tolerances, slight deviations from a perfectly symmetric sensor layout occur. This becomes evident from the disturbances emerging in the simulated differential output signal of the two sense masses depicted in Figs. 7a and 7b. By the aid of an adaptive control loop these disturbances will be eliminated.

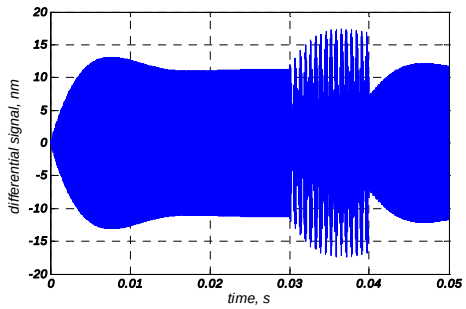

Fig. 7a: Differential output signal of the two sense masses. Impact of the first vibrational eigenmode of the PSOIC housing.

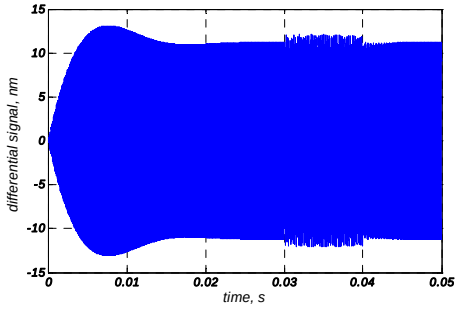

Fig. 7b: Differential output signal of the two sense masses. Impact of the first vibrational eigenmode of the QFP housing.

CONCLUSIONS

We presented a high-level model of a dual gimbaled mass gyroscope that combines computational efficiency with physical transparency on system level, providing a realistic description of the dynamic behavior under real-world operating conditions. Exemplary investigations showing the impact of housing vibrations on the sensor output signal demonstrate the practicality of our approach. It thus provides the proper basis for on-going research activities focusing on the design of control algorithms, which minimize or even eliminate the impact of the most prominent environmental or internal, manufacturing-induced disturbances on the sensor system and, thus, helps to significantly enhance the quality of signal conditioning.

REFERENCES

[1] R. Khalilyulin, F. Salwetter, G. Wachutka: Coupled Package-Device Modeling of an Angular Rate Gyroscope. Book of Abstracts of 18th Micromechanics Europe Workshop (MME 2007), Guimaraes, Portugal, Sept. 16-18, 2007, pp. 297-300.

[2] T. Veijola: Compact Damping Models for Lateral Structures Including Gas Rarefaction Effects. Proceedings of MSM 2000, San Diego, CA, March 27-29, 2000, pp. 162-165.

[3] G. Schrag, G. Wachutka: Physically-Based Modeling of Squeeze Film Damping by Mixed Level System Simulation. Sensors and Actuators A: vol. A97-98 (2002), pp. 193-200.

[4] B.J. Hamrock, Fundamentals of Fluid Film Lubrication, McGraw-Hill, 1994.

[5] R. Khalilyulin, G. Wachutka: Adaptive Control for Reducing the Impact of Damping Effects on the Output Signal of Microgyroscopes. Proc. of the 20th European Conference on Solid-State Transducers (EUROSENSORS 2006), Göteborg, Sweden, Sept. 17-20, 2006, pp.100-101.